Available online at BCREC Website: https://bcrec.undip.ac.id

Bulletin of Chemical Reaction Engineering & Catalysis, 13 (1) 2018, 119-126

Research Article

Enhanced Photocatalytic Activity of La^{3+} doped Bicrystalline Titania Prepared via Combustion method for the Degradation of Cationic dye Under Solar Illumination

Radhika R. Nair[1], Mothi Krishna Mohan[2], K.R. Sunajadevi[1]*

[1]Department of Chemistry, Christ University, Bangalore-560029, Karnataka, India
[2]Department of Sciences & Humanities, Christ University, Bangalore-560074, Karnataka, India

Received: 28th July 2017; Revised: 19th October 2017; Accepted: 30th October 2017;
Available online: 22nd January 2018; Published regularly: 2nd April 2018

Abstract

La^{3+} doped TiO_2 photocatalysts were successfully synthesized by combustion method in the presence of urea and were characterized by various physico-chemical techniques. Further, the photocatalytic performance of the synthesized catalysts was monitored by photocatalytic degradation of synthetic cationic dye-Methylene Blue (MB) under solar illumination. The bicrystalline phase of anatase and rutile was confirmed by X-ray diffraction analysis. Moreover, the transformation from anatase to rutile phase proceeds at a slower rate in the La^{3+} doped TiO_2 catalysts. Effective separation of charge carriers, a synergistic effect in the bicrystalline framework of anatase and rutile, smaller crystallite size, and higher concentration of surface adsorbed hydroxyl groups helped these catalysts to show improved activity for the dye degradation.

Keywords: Titania; La^{3+} doped titania; combustion synthesis; photocatalysis; degradation of cationic dye

How to Cite: Nair, R.R., Mohan, M.K., Sunajadevi, K.R. (2018). Enhanced Photocatalytic Activity of La^{3+} doped Bicrystalline Titania Prepared via Combustion method for the Degradation of Cationic dye Under Solar Illumination. *Bulletin of Chemical Reaction Engineering & Catalysis*, 13 (1): 119-126 (doi:10.9767/bcrec.13.1.1427.119-126)

Permalink/DOI: https://doi.org/10.9767/bcrec.13.1.1427.119-126

1. Introduction

Heterogeneous photocatalysis with TiO_2 in presence of sunlight is a developing technology for removing organic pollutants from atmosphere and waste water. The application of titanium dioxide has been widely focused on the photosensitive behavior and exploited in several applications concerning the environmental field and solar cells [1]. Because of the strong redox capacity, chemical inertness, cost effectiveness and bio-compatibility, titanium dioxide has been considered as the superior semiconductor photocatalyst [2]. However, the overall efficiency of TiO_2 is limited to the UV region, which is only four percentage of the solar energy reaching the surface of earth. The TiO_2 can utilize a small part of the solar spectrum for photocatalytic activity due to its wide band gap. In recent years, the major challenge in photocatalysis is to widen the absorption spectrum of titanium diox-

* Corresponding Author.
E-mail: sunajadevi.kr@christuniversity.in (Sunajadevi, K.R.)
Tel: +91 80 40129310; Fax: +91 80 40129000

ide to the higher wavelength region [3-5]. The major drawback in photocatalysis is low quantum yield. Numerous works reported suggests that the key to widen the spectral range of absorption of titania is by doping it with various metal ions..

Different concentration of various metal ions (Al^{3+}, Cr^{3+}, Si^{4+}, ZnO, CeO_2, Ta^{5+}, Nb^{5+}, Sb_2O_5, PO_4^{3-}, SO_4^{2-}, Cl^-, Pt) as dopants on titania has been reported by various researchers [6-11]. These dopants act as electron traps and reduce the rate of recombination, which helps in the displacement of the absorption of TiO_2 to the visible region. This is due to the increase in the concentration of organic pollutants at the surface of the catalyst. Functional groups present in the organic pollutants interact with the *f* orbitals of rare earth ion, resulting in increased photoactivity [12-15]. Lin *et al.* [16] showed that mixtures of titania with La_2O_3 or Y_2O_3 exhibit enhanced photoactivity towards the oxidation of acetone. Xu *et al.* [17] have used sol-gel method to prepare different rare earth doped TiO_2 and found that the amount of rare earth was an important factor affecting photocatalytic activity. Xie *et al.* [18] explained the Nd^{3+} doped titania sol for the higher visible light photoactivity. Higher activity for the degradation of p-chlorophenoxy acetic acid has been studied over Eu^{2+}, Yb^{3+}, Pr^{3+} doped titania [12]. Sm^{3+} doping leads to considerable modification in the photo catalytic activity of TiO_2 for cango red dye degradation under visible light [19]. Sun *et al.* [20] reported a decrease in band gap after doping rutile titania by Pt. Recently, the mixed phase of anatase and rutile is shown to exhibit higher photo activity compared to the pure anatase or rutile phase. This is due to the synergistic effect between these two phases [21].

In recent years, combustion synthesis has been used as a versatile method for the synthesis of catalyst. Compared to other methods, there are some obvious advantages in combustion method as they can be easily repeated, the reaction is safe and quick, no complicated experimental procedures and are environment-friendly. But to the best of our knowledge, no literature is found on the synthesis of La^{3+} modified titania by combustion method. Nevertheless, the aim of the present work is to synthesize the La^{3+} doped TiO_2 catalyst by combustion method and to investigate its photocatalytic activity over the photodegradation of MB dye under illumination of solar light.

2. Materials and Methods

2.1 Materials

Titanium tetra isopropoxide ($Ti\{OCH(CH_3)_2\}_4$, Sigma Aldrich) named as TTIP, Lanthanum nitrate ($La(NO_3)_3.6H_2O$, Merck Chemicals), Glycine ($C_2H_5NO_2$, Merck Chemicals), and Methylene Blue (BDH) were used without further purification.

2.2 Catalyst preparation

TiO_2 nanoparticle was prepared by combustion synthesis method [22]. TTIP and glycine in 5:1 ratio was mixed well transferred into a crucible and fired at 500 ^oC in a pre heated muffle furnace for 4 hours. Glycine was used as an organic fuel during the process. In a mortar, required amount of lanthanum nitrate and glycine were mixed and to this mixture TTIP is added drop wise. It was transferred into a crucible and was placed in a 500 ^oC pre heated muffle furnace for 4 hours. The La^{3+} doping was done using different mol percentages like 0.5, 1, and 2. The combusted puffy and porous powder obtained was sieved and named as $0.5LaTiO_2$, $1LaTiO_2$ and $2LaTiO_2$, respectively.

2.3 Catalyst characterization

The crystallite phase of the catalysts and variation of lattice parameter upon doping with La^{3+} ions were determined by X-ray diffraction (XRD) measurements using PANalytical Xpert Pro X-ray Diffractometer using Cu-Kα radiation (λ = 0.154 nm) at 40 kV, at a scanning rate of 2° min^{-1}. The specific surface area of the powders was measured by Brunauer Emmett Teller (BET) method in which N_2 gas was adsorbed at 77 K using Micromeritics Gemini surface area analyzer using nitrogen as an adsorbate. EDX and SEM analysis were carried out in Quanta ESCM, FEI instrument to obtain compositional information of the metal ions incorporated into the TiO_2 lattice and surface morphology respectively. Light response of the catalysts were recorded in the range of 200-900 nm on Labomed UV-Vis double beam UVD-500 spectrophotometer with a CCD detector, using $BaSO_4$ as reflectance standard. Kubelka-Munk method was used to calculate the band gaps of the photocatalysts. Temperature programmed desorption of ammonia (NH_3-TPD) was used to determine the total acidity of the sample.

2.4 Measurement of photocatalytic properties: degradation of methylene blue

The photocatalytic activity of titania and modified titania were evaluated via the degradation of MB in aqueous solution under solar irradiation. The photocatalyst (0.20 g) was added into a 100 mL (2.80×10^{-5} MB) solution. The suspension was stirred in dark for 30 minutes in order to reach the adsorption-desorption equilibrium. Photocatalytic activity was performed between 11 am and 2 pm during the summer season in Bangalore, India, having latitude 12.9667^0 N and longitude 77.566^0 E. The average intensity of sunlight was 12.76 W/m^2. A convex lens was used to concentrate the solar light and the reaction mixture was exposed to this concentrated solar light. To compare the photocatalytic activity of all the catalysts, the experiments were simultaneously conducted to avoid the error arising due to the fluctuations in solar intensity (At this time interval the fluctuation in solar intensity was minimum). The filtrates collected at different time intervals were analyzed by UV-vis spectroscopic technique using a Shimadzu UV-Vis 1800 Spectrophotometer from 400 to 800 nm.

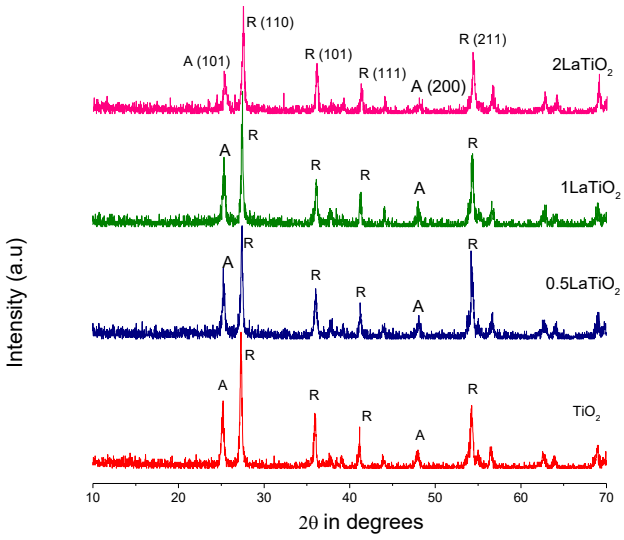

Figure 1. XRD pattern of (a) TiO_2, (b) $0.5LaTiO_2$, (c) $1LaTiO_2$, (d) $2LaTiO_2$ (A-Anatase (JCPDS Card no. 21-1272), R-Rutile (JCPDS Card no. 21-1276))

3. Results and Discussion

3.1 Catalyst characterization

Figure 1 depicts the X-ray diffraction (XRD) patterns of TiO_2 and doped TiO_2. XRD results showed that mixtures of anatase and rutile phase are seen in all the samples. The peaks at 2θ = 25.3° (101), 48.1° (200) and 37.7° (004) represent anatase form of TiO_2 while those at 2θ = 27.4° (110), 54.2° (211) and 41.2° (111) are the characteristics of the rutile phase. The Spurr and Meyer's equation [23] ($X_R = (1+0.8I_A/I_R)^{-1}$) is used to estimate the percentage (X_R) of the rutile phase, where I_A and I_R represents the intensity of the anatase peak at 2θ = 25.3° and rutile peak at 2θ =27.4°. Moreover, the average crystallite size was calculated using Scherer's equation [24] ($D = k\lambda / \beta \cos\theta$), where D is the crystalline size (nm), k is the shape factor and is equal to 0.9, λ is the wavelength of the X-rays (0.15418 nm); β is the linewidth at the half maximum of the anatase (at 2θ = 25.3°) or of the rutile (at 2θ = 27.4°) peak and θ is the diffraction angle. The solid surface can be estimated using the following relation: ($S = 6/\rho D$), where ρ is the density of TiO_2 (anatase = 3.84 g.cm^{-3} and rutile = 4.13 g.cm^{-3}) and D is the crystallite size (mm) [25]. The results are tabulated in Table 1. Further, the La^{3+} ion effectively hinders the growth of crystallite size and hence suppresses the transformation of anatase to rutile phase. Relative ratio of rutile to anatase is reduced with lower lanthanum content. No peaks corresponding to lanthanum was observed in any of the doped titania which may be due to its low concentration.

Table 1. Results of XRD analysis of the catalysts

Catalysts	2θ (degrees)		*d* spacing (Å)		Phase composition	Lattice parameters (Å)		Crystallite size (nm)	Solid surface (m^2.g^{-1})
	A*	R*	A	R	A:R	a=b	c	A:R	R
TiO_2	25.3	27.3	3.53	3.26	28:72	4.610	2.958	27:36	40.3
$0.5LaTiO_2$	25.3	27.4	3.53	3.26	32:68	4.610	2.958	26:31	46.9
$1LaTiO_2$	25.3	27.4	3.53	3.26	29:71	4.610	2.958	17:29	50.1
$2LaTiO_2$	25.3	27.5	3.53	3.26	21:79	4.610	2.958	27:26	55.8

A*-Anatase 101 plane, R*-Rutile 110 plane

The lattice parameters calculated (Table 1) using the Bragg's equation, (d_{hkl} = l/2 *sin* θ), indicates that there is no change in these values after doping. This indicates that La^{3+} could not enter the titania lattice due to the large ionic radii of La^{3+} compared to Ti^{4+}. Further, the XRD patterns are composed of a significant amount of rutile phase and sharp intense peaks depicts the crystalline nature of the modified sample. Introduction of larger 'La' ions induces strain energy in the crystal, which inhibits the phase transition from anatase to rutile.

The existence of Ti, La, and O elements on the prepared sample was vindicated by EDX spectroscopy analysis. It is also useful to detect the traces of other materials such as dopants or adducts. The intensity of the peaks is directly related to the amount of elements present in the sample. Atom percentage of each and every element present in the modified samples was calculated and tabulated (Figure 2). This confirmed the successive incorporation of dopants into the TiO_2 system.

The morphology of the prepared catalysts was investigated using SEM images (Figure 3).

Table 2. BET surface area and pore volume of the catalysts

Catalyst	BET surface area (m^2/g)	Pore Volume (10^{-6} m^3/g)	Pore diameter (10^{-9} m)
TiO_2	58.8	0.10	6.8
0.5La TiO_2	98.3	0.14	5.7
1La TiO_2	82.4	0.20	9.7
2La TiO_2	73.0	0.22	12.1

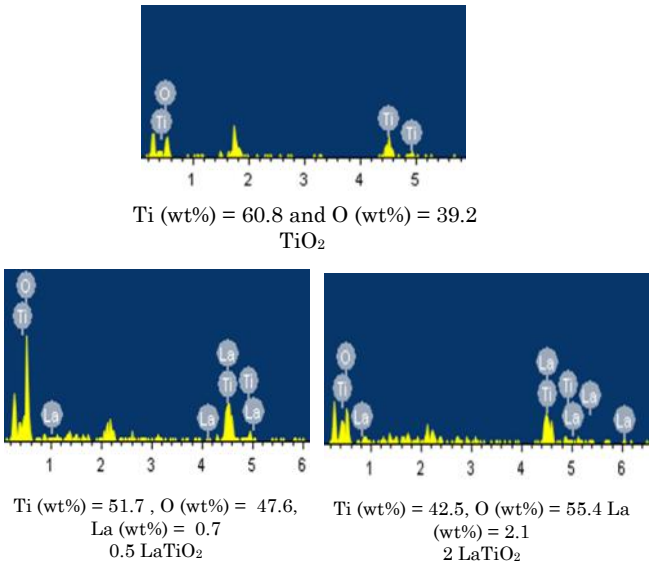

Figure 2. EDAX results of the prepared catalysts

The catalyst morphology influences the light absorption ability and generation of excited ions, which in turn gets reflected in its efficiency. The prepared samples consist of nearly spherical particles with some degree of aggregation. The shapeless structures in the image are mainly due to aggregation which may occur during solution combustion synthesis. Spherical particles enhanced the surface area of the prepared system which in turn improved the activity.

Surface areas of modified samples were found to be high compared to bare sample. The results are tabulated in Table 2. Lower crystallite size and nucleation sites introduced by dopants are the major reasons for high surface area of the modified systems. Average pore diameter is calculated using the formula (d = $4V_p/S_p$) (assuming the pores are cylindrical), where V_p is the pore volume, S_p is the surface area, and d is the average pore diameter. Pore

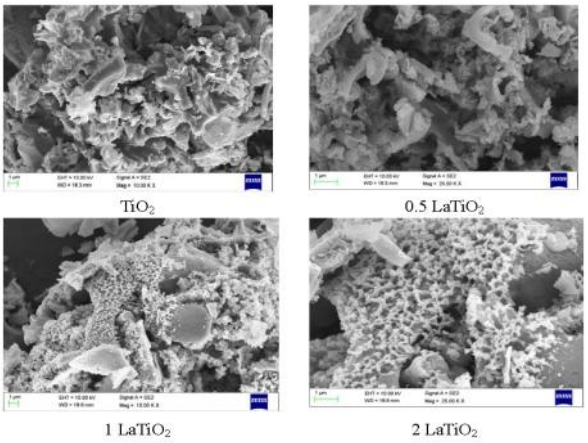

Figure 3. Scanning electron microscopy images of the prepared catalysts

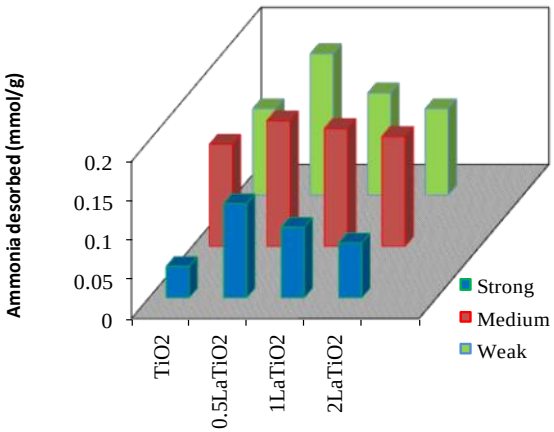

Figure 4. Amount of ammonia desorbed by NH_3-TPD (mmol. g^{-1})

diameter increases as the metal ion concentration increases on titania surface.

Temperature programmed desorption (TPD) of ammonia serves as a dependable technique for the determination of the number and distribution of acid sites in the specified temperature range. The NH_3-TPD results show (Figure 4) an increased amount of total acidic sites for La^{3+} doped titania compared to bare titania. This shows the availability of adsorption sites in the modified samples, making them more efficient catalysts.

Figure 5 shows the UV Visible Diffuse reflectance spectra of the bare and modified sample. Light absorption of pristine sample is in the UV region, but the spectral response of modified sample shows a red shift in absorption maximum. The band gap of the bare titania and $0.5LaTiO_2$ sample was calculated by the equation (E_g = 1,239.8/λ) and were found to be 3.1 eV and 2.8 eV, respectively [26]. This is one of the simple versions of Kubelka-Munk equation where 'λ' is the wavelength from which reflection has taken place. The red shift (Figure 5) in the optical absorption band is due to the presence of La^{3+} ions, and it can be attributed to a charge-transfer transition between the lanthanide *f* electrons and the conduction or valence band of the titania [27]. A larger red shift indicates that the sample can absorb more photons in the visible region.

3.2 Catalytic activity towards the degradation of methylene blue

Solar light induced photocatalytic activity of the samples was evaluated by investigating the kinetics of the degradation reaction of methylene blue in aqueous suspensions. After stirring the MB solution and the photocatalysts (200 mg) in the dark for 30 minutes, the reaction has been carried out. The amount of adsorption was calculated by comparing the concentration of the MB dye before and after stirring. The percentage of dye adsorption was calculated using the formula: (C_o-C)/C_o×100%), where C_0 is the initial and C is the residual concentrations of MB and the values of dye adsorption are as follows: 5.3% (TiO_2), 8.7% ($0.5LaTiO_2$), 7.4% ($1LaTiO_2$), and 6.4% ($2LaTiO_2$). A first-order kinetic model was used to compare the reaction rate among different catalysts ($ln\ C_0 = kt + ln\ C$) where C is the MB concentration at time t, k is the apparent reaction rate constant and C_0 is the initial concentration. A plot of $ln\ C_0/C$ with respect to time t is plotted (Figure 6) to evaluate the rate constant. We assume that concentration of MB after attaining the desorption-adsorption equilibrium is the initial concentration C_0.

According to this kinetic model, the rate constants, k, were found to be 0.0009, 0.0023, 0.0021, 0.0016 min^{-1} for TiO_2, $0.5LiTiO_2$, $1LaTiO_2$, $2LaTiO_2$, respectively. From these values, it is understood that the solar light reactivity of TiO_2 is significantly enhanced by La^{3+}, especially for $0.5LaTiO_2$ catalyst. Not only the surface area but the synergistic effect of anatase and rutile phase could also be responsible for enhancement photocatalytic activity under visible light irradiation.

In the present study, doped and undoped titania show bicrystalline frameworks of anatase and rutile. All the catalysts showed good activity and the percentage degradation of MB increases after La^{3+} doping. The enhanced activity of the modified titania can be explained due

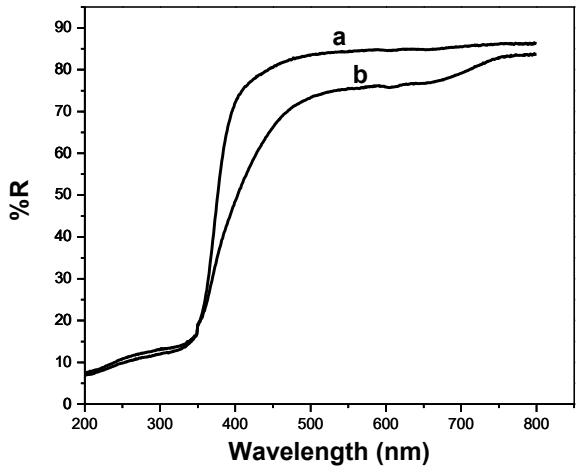

Figure 5. UV-DRS spectra of a) TiO_2, b) $0.5LaTiO_2$

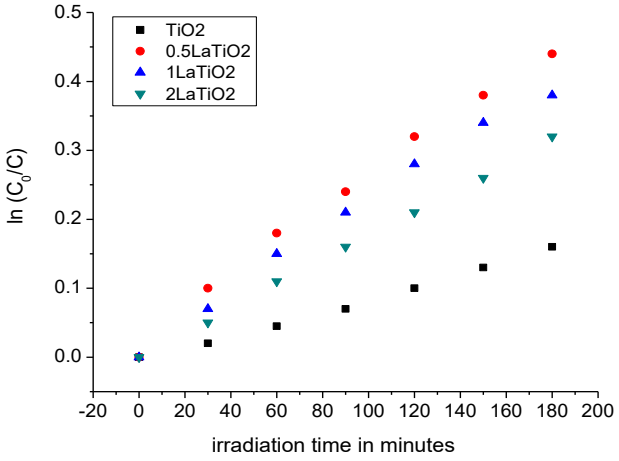

Figure 6. $ln(C_0/C)$ versus time plot of MB degradation under solar irradiation for different catalysts

to the higher adsorption of MB. Moreover, it can be attributed to the formation of Lewis acid-base complexes between the MB and La^{3+} ions. La^{3+} dopant decrease the crystallite size (Table 1) which facilitates the absorption for MB. Doping had increased oxygen vacancies and/or surface defects in the TiO_2 surface which helps in capturing photoelectrons and inhibits the recombination between photo electrons and holes and results in enhanced quantum efficiency [28]. The band gap of rutile is highly favorable for visible light excitation. The proposed charge transfer mechanism for our work is given in Figure 7. Under solar light excitation, the photogenerated electron from the CB of rutile transfers to trapping sites of the anatase phase, which can be considered as an antenna effect by the rutile phase [29].

Our report suggests that $0.5LaTiO_2$ shows the improved photo reactivity, which may be in favour of the most efficient separation of the charge carriers. The value of the space charge region potential for the efficient separation of electron-hole pairs must be not lower than 0.2 V. The space charge region becomes very narrow when the concentration of doping ions is very high. This alters the penetration depth of light into TiO_2 and exceeds the space charge layer; which in turn makes the recombination of the photo generated electron–hole pairs in semiconductor easier. Therefore, there is an optimum concentration of dopant ions to make the thickness of space charge layer substantially equal to the light penetration depth. Excess amounts of lanthanum ion covering the surface of TiO_2 would increase the number of recombination centers and result in low photoactivity. So, $LaTiO_2$ with more than 0.5 wt% show poor photocatalytic activity. The photogenerated electrons could easily transfer from the interior to the surface of the catalyst, which would promote photocatalytic reaction. On the basis of the above analysis, it is suggested that the enhanced photocatalytic activity of La^{3+} doped TiO_2 could be a synergetic effect of many factors, including red shifts to longer wavelengths, polycrystalline phase and enhanced rates of interfacial charge transfer [30].

4. Conclusions

In conclusion, we have developed cost effective, recyclable, and environmentally benign La^{3+} doped TiO_2 by solution combustion method. The synthesized catalyst has been identified with bicrystalline phase (anatase and rutile) having crystallite size of 20-35 nm. Moreover, a red shift in the absorption of modified titania is evidenced from diffuse reflectance spectroscopy. Subsequently, these catalysts have been investigated for the photodegradation of MB under solar light and proved to be an efficient photocatalyst for the treatment of MB cationic dye. The degradation efficiency has been remarkably increased and is strongly dependent on adsorption of the dyes on the catalyst surface. It is concluded that the synergic effect, small particle size and the separation of charge carriers (e^-/h^+) have a major effect on photocatalytic activity of these materials. Hence, our results indicate the poten-

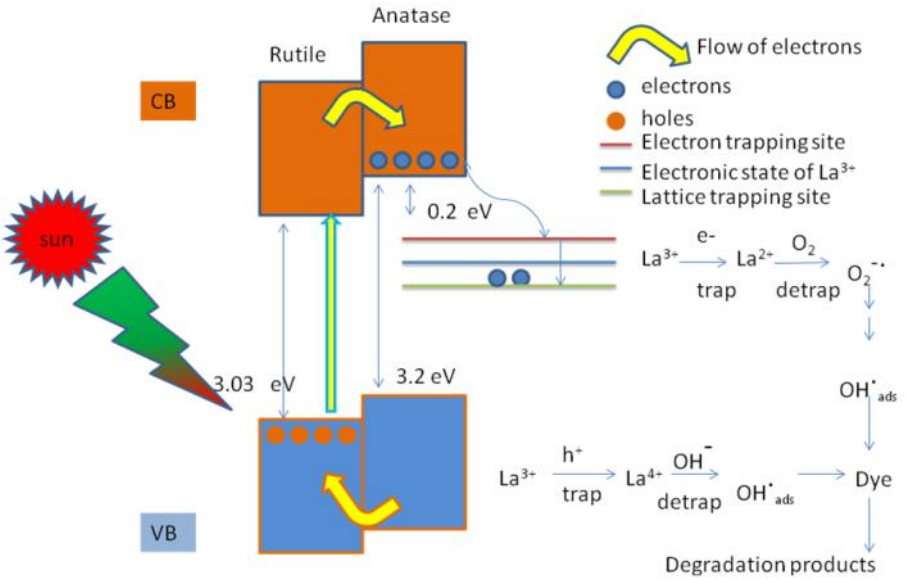

Figure 7. Charge transfer under solar light for La^{3+} doped bicrystalline titania

tial use of these materials in real wastewater treatment.

Acknowledgment

Authors gratefully acknowledge Christ University for the facilities to carry out this work and also thankful to St Joseph's College, Bangalore and IISc Bangalore for analysis.

References

[1] Mills, A., Le, Hunte S. (1997). An overview of semiconductor photocatalysis, *J. Photochem. Photobio. A: Chem*., 108: 1-35.

[2] Fox, M. A., Dulay, M. T. (1993). Heterogeneous Photocatalysis, *Chem. Rev*., 93: 341-357.

[3] Wang, Z., Liu, X., Li, W., Wang, H., Li, H. (2014). Enhancing the photocatalytic degradation of salicylic acid by using molecular imprinted S-doped TiO_2 under simulated solar light, *Ceramics International,* 40: 8863-8867.

[4] Zhang, Y., Cheng, K., Lv, F., Huang, H., Fei, B., He, Y., Ye, Z., Shen, B. (2014). Photocatalytic treatment of 2,4,6-trinitotoluene in red water by multi-doped TiO_2 with enhanced visible light photocatalytic activity**,** *Colloids Surf. A Physicochem. Eng. Asp,* 452: 103-108.

[5] Lin, Y. T., Weng, C. H., Chen, F. Y. (2014). Key operating parameters affecting photocatalytic activity of visible-light-induced C-doped TiO_2 catalyst for ethylene oxidation*, Chem. Eng. J*., 248: 175-183.

[6] Yang, Y., Ferreira, J. M. F. (1998). Inhibitory Effect of the Al_2O_3 – SiO_2 Mixed Additives on the Anatase – Rutile Phase Transformation, *Mater. Letters,* 36: 320-324.

[7] Guidi, V., Carotta, M. C., Ferroni, M., Martinelli, G., Sacerdoti, M. (2003). Effect of Dopants on Grain Coalescence and Oxygen Mobility in Nanostructured Titania Anatase and Rutile, *J Phys. Chem. B*, 107: 120-124.

[8] Sunajadevi, K. R., Sugunan, S. (2004). Synthesis, characterization and benzylation activity of nanocrystalline chromia loaded sulfated titania prepared via the sol gel route, *Catal. Commun.,* 5: 575-581.

[9] Francisco, M. S. P., Mastelaro, V. R. (2002). Inhibition of the Anatase-Rutile Phase Transformation with Addition of CeO_2 to CuO-TiO_2 System: Raman Spectroscopy, X-ray Diffraction, and Textural Studies, *Chem. Mater,* 14: 2514-2518.

[10] Shannon, R. D., Pask, J. A. (1965). Kinetics of the Anatase-Rutile Transformation, *J Am. Ceram. Soc*, 48: 391-398.

[11] Sanchez, E., Lopez, T., Gomez, R., Bokhimi, X., Morales, A., Novaro, O. (1996). Synthesis and Characterization of Sol-Gel Pt/TiO_2, *J. Solid State Chem,* 122: 309-314.

[12] Ranjit, K.T., Willner, I., Bossmann, S. H., Braun, A. M. (2001). Lanthanide Oxide-Doped Titanium Dioxide Photocatalysts: Novel Photocatalysts for the Enhanced Degradation of *p*-Chlorophenoxyacetic Acid, *Environ Sci. Technol,* 35: 1544-1549.

[13] Zhang, Y., Xu, H., Xu, Y., Zhang, H., Wang Y. (2005). The effect of lanthanide on the degradation of RB in nanocrystalline Ln/TiO_2 aqueous solution**,** *J. Photochem. Photobiol. A Chem.,* 170: 279-285.

[14] Zhang, Y. H., Zhang, H. X., Zu, Y. X., Wang Y. G. (2003). Europium doped nanocrystalline titanium dioxide: preparation, phase transformation and photocatalytic properties, *J. Mater. Chem*., 13: 2261-2265.

[15] Huang, D. W., Lee, J. S., Li, W., Oh, S. H. (2003). Electronic Band Structure and Photocatalytic Activity of $Ln_2Ti_2O_7$ (Ln = La, Pr, Nd), *J. Phys. Chem. B,* 107: 4963-4970.

[16] Lin, J., Yu J. C. (1998). An investigation on photocatalytic activities of mixed TiO_2-rare earth oxides for the oxidation of acetone in air, *J. Photochem. Photobiol. A Chem.,* 116: 63-67.

[17] Xu, A. W., Gao, Y., Liu, H. Q. (2002). The Preparation, Characterization, and their Photocatalytic Activities of Rare-Earth-Doped TiO_2 Nanoparticles , *J. Catal.,* 207: 151-157.

[18] Xie, Y., Yuan, C., Li, X. (2005). Photocatalytic degradation of X-3B dye by visible light using lanthanide ion modified titanium dioxide hydrosol system**,** *Colloid Surf. A Physicochem. Eng. Asp.,* 252: 87-94.

[19] Xie, Y., Yuan, C., Li, X. (2005). Photosensitized and photocatalyzed degradation of azo dye using Ln^{n+}-TiO_2 sol in aqueous solution under visible light irradiation**,** *Mater. Sci. Eng. B*, 117: 325-333.

[20] Sun, B., Sminiorstis, P. G., Boolchand, P. (2005). Synthesis, characterization and photocatalytic activity of Li-, Cd-, and La-doped TiO_2, *Langmuir*, 211: 11397-11403.

[21] Gomathi Devi, L., Nagaraju, K., Girish Kumar S. (2009). Preparation and Characterization of Mn-Doped Titanates with a Bicrystalline Framework: Correlation of the Crystallite Size with the Synergistic Effect on the Photocatalytic Activity , *J. Phys. Chem. C.,* 113: 15593-15601.

[22] Radhika, R. N., Arulraj, J., Sunaja Devi, K. R. (2016 Ceria doped titania Nano particles: Synthesis and Photo Catalytic Activity, *Mat. Today. Proc*., 6 (3): 1643-1649.

[23] Spurr, R., Myers W. (1957). Quantitative Analysis of Anatase-Rutile Mixtures with an X-Ray Diffractometer, *Anal. Chem.,* 29: 760-762.

[24] Scherrer, P. (1918). Bestimmung der Gröss Kolloidteilchen Mittels hrichten von der Gesellschaft der Wissenschaften, Göttingen, *Mathematisch-Physikalische Klasse*, 2: 98-100.

[25] Elsellami, L., Lachheb, H., Houas A. (2015). Synthesis, characterization and photocatalytic activity of Li-, Cd-, and La-doped TiO_2, *Mater. Sci. Semicondu. Proce*., 36: 103-114.

[26] Kubelka, P., Munk F. (1931). Photocatalysis: fundamentals and applications, *Tech. Phys.,* 12: 593-601.

[27] Borgarello, E., Kiwi, J., Gratzel, M., Pelizzetti, E., Visca M. (1982). Visible light induced water cleavage in colloidal solutions of chromium-doped titanium dioxide particles, *J Ameri. Chem. Soc.*, 104: 2996-3002.

[28] Huo, Y., Zhu, J., Li, J., Li, G., Li, H. (2007). An active La/TiO_2 photocatalyst prepared by ultrasonication-assisted sol–gel method followed by treatment under supercritical conditions, *J. Mol. Catal. A Chem*. 278: 237-243.

[29] Hurum, D. C., Agrios, A. G., Gray, K. A., Rajh, T., Thurnauer M. C. (2003). Explaining the Enhanced Photocatalytic Activity of Degussa P25 Mixed-Phase TiO_2 Using EPR, *J. Phys. Chem. B*, 107: 4545-4549.

[30] Hassan, M.S, Amna T., Yang O B., Kim H.C., Khil M.S. (2012). TiO_2 nanofibers doped with rare earth elements and their photocatalytic activity, *Ceramics International*, 38: 5925-5930.

[31] Poh, N.E., Nur, H., Muhid, M.N.M., Hamdan, H. (2006). Sulphated AlMCM-41: Mesoporous solid Brønsted acid catalyst for dibenzoylation of biphenyl. *Catal. Today*. 114(2-3): 257-262.

[32] Leofanti, G., Padovan, M., Tozzola, G., Venturelli, B. (1998). Surface area and pore texture of catalysts. *Catal. Today,* 41(1-3): 207-219.

[33] Walker, J. (1986). Coal derived carbons. *Carbon*, 24(4): 379-386.